DOI: 10.1002/chem.200701878

Oxidative Double Dehalogenation of Tetrachlorocatechol by a Bio-Inspired Cu^{II} Complex: Formation of Chloranilic Acid

Pieter C. A. Bruijnincx,[a] Marta Viciano-Chumillas,[b] Martin Lutz,[c] Anthony L. Spek,[c] Jan Reedijk,[b] Gerard van Koten,[a] and Robertus J. M. Klein Gebbink*[a]

Abstract: Copper(II) complexes of the potentially tripodal N,N,O ligand 3,3-bis(1-methylimidazol-2-yl)propionate (L1) and its conjugate acid HL1 have been synthesised and structurally and spectroscopically characterised. The reaction of equimolar amounts of ligand and Cu^{II} resulted in the complexes $[Cu(L1)]_n(X)_n$ ($X = OTf^-$, PF_6^-; $n = 1,2$), for which a new bridging coordination mode of L1 is inferred. Although these complexes showed moderate catecholase activity in the oxidation of 3,5-di-*tert*-butylcatechol, surprising reactivity with the pseudo-substrate tetrachlorocatechol was observed. A chloranilato-bridged dinuclear Cu^{II} complex was isolated from the reaction of $[Cu(L1)]_n(PF_6)_n$ with tetrachlorocatechol. This stoichiometric oxidative double dehalogenation of tetrachlorocatechol to chloranilic acid by a biomimetic copper(II) complex is unprecedented. The crystal structure of the product, $[Cu_2(ca)Cl_2(HL1)_2]$, shows a bridging bis-bidentate chloranilato (ca) ligand and ligand L1 coordinated as its conjugate acid (HL1) in a tridentate fashion. Magnetic susceptibility studies revealed weak antiferromagnetic coupling ($J = -35\ cm^{-1}$) between the two copper centres in the dinuclear complex. Dissolution of the green complex $[Cu_2(ca)Cl_2(HL1)_2]$ resulted in the formation of new pink-purple mononuclear compound $[Cu(ca)(HL1)(H_2O)]$, the crystal structure of which was determined. It showed a terminal bidentate chloranilato ligand and N,N-bidentate coordination of ligand HL1, which illustrates the flexible coordination chemistry of ligand L1.

Keywords: bioinorganic chemistry · copper · dehalogenation · hydrogen bonds · N,O ligands

Introduction

Copper-containing metalloenzymes play a major role in the activation of dioxygen in nature.[1] Currently, up to seven different types of copper sites in proteins can be discerned on the basis of structure and spectroscopy of their active site, and they feature mono-, di-, tri- or tetranuclear copper centres.[2] The type-3 active sites of copper proteins, for instance, consist of two copper(II) ions in close proximity, both of which are coordinated by three histidine residues. These type-3 sites in copper proteins are represented by haemocyanin, tyrosinase, and catechol oxidase, all of which have now been characterised crystallographically.[3–5] Haemocyanin reversibly binds dioxygen for transport, whereas the other proteins are enzymes that are involved in the oxidation of phenols to catechols (tyrosinase) and subsequent two-electron oxidation of the catechols to quinones (both tyrosinase and catechol oxidase). To understand the mechanisms by which these closely related enzymes catalyse their respective transformations, many structural and functional modelling studies have been reported. Most of these deal with model compounds of catechol oxidase,[6–11] and they have recently been reviewed.[2]

Some of us earlier reported copper[12,13] and iron[14,15] complexes of the family of monoanionic, substituted 3,3-bis(1-alkylimidazol-2-yl)propionate ligands as biomimetic oxidation catalysts. Homogeneous and immobilised copper(II) complexes of parent ligand L1 (Figure 1) have, for instance, been tested in the oxidation of benzyl alcohol.[13] Whereas a

[a] Dr. P. C. A. Bruijnincx, Prof. Dr. G. van Koten, Prof. Dr. R. J. M. Klein Gebbink
Chemical Biology & Organic Chemistry
Department of Chemistry, Faculty of Science, Utrecht University
Padualaan 8, 3584 CH Utrecht (The Netherlands)
Fax: (+31) 30-252-3615
E-mail: r.j.m.kleingebbink@uu.nl

[b] M. Viciano-Chumillas, Prof. Dr. J. Reedijk
Leiden Institute of Chemistry, Leiden University
P. O. Box 9502, 2300 RA Leiden (The Netherlands)

[c] Dr. M. Lutz, Prof. Dr. A. L. Spek
Bijvoet Centre for Biomolecular Research, Crystal and Structural Chemistry
Department of Chemistry, Faculty of Science, Utrecht University
Padualaan 8, 3584 CH Utrecht (The Netherlands)
E-mail: a.l.spek@chem.uu.nl

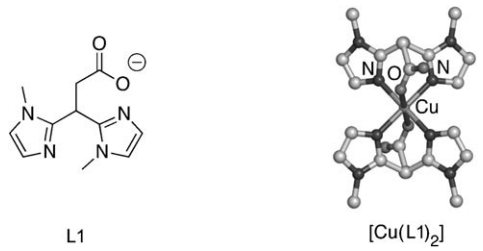

Figure 1. Ligand L1 and 2:1 ligand/metal complex $[Cu(L1)_2]$.[12]

1:1 ligand to copper complex was found inside a zeolite framework,[13] we mainly observed 2:1 species $[Cu(L1)_2]$ in solution and single-crystal X-ray diffraction studies (Figure 1).[12]

We have now expanded these studies on the coordination chemistry of L1 with copper(II) ions. A study of the catecholase activity of these complexes resulted in the unexpected and unprecedented formation of chloranilic acid from tetrachlorocatechol. This observation has environmental relevance. Tetrachlorocatechol is part of a bigger group of pollutants, such as chlorinated phenols, guaiacols (2-methoxyphenols) and catechols, that are found in the low-molecular weight fraction of waste generated by, for instance, the paper bleaching industry.[16,17] These highly chlorinated organic compounds include some of the most toxic and persistent organic pollutants. A copper-mediated oxidative dehalogenation reaction that provides a new approach to the chemical degradation of these pollutants is described herein.

Results

Synthesis of copper(II) complexes: The coordination chemistry of L1 towards copper(II) ions was found to be stoichiometry dependent, as was previously observed for other transition metal cations, such as zinc(II).[18] Earlier, we reported complex $[Cu(L1)_2]$ (Figure 1), which can be obtained by the addition of two equivalents of L1 to a copper(II) source.[12] However, a different complex is obtained when only one equivalent of L1 is used. The reaction of equimolar amounts of $Cu(OTf)_2$ and K[L1] resulted in the isolation of a light blue complex. According to elemental analysis, a complex of stoichiometric amounts of copper(II), ligand and anion is formed, which we label as [**1**](OTf) (see below).

Previous studies showed that the positions of the symmetric and asymmetric carboxylato stretching vibrations in the IR spectrum are indicative of the binding mode of the ligand.[12,18] The IR spectrum of the precipitated product from the 1:1 reaction of $Cu(OTf)_2$ and L1, however, showed a distinct absorption pattern that had not previously been observed. The asymmetric and symmetric stretching vibrations were found at 1555 and 1433 cm^{-1}, respectively. As a result, $\tilde{\nu}_{as}-\tilde{\nu}_{s}$ is only 122 cm^{-1}. This is substantially less than $(\tilde{\nu}_{as}-\tilde{\nu}_{s})_{ionic}$ (188 cm^{-1}) and points to a bridging carboxylato group.[19] Furthermore, the four sharp bands observed at 1259, 1224, 1148 and 1028 cm^{-1} are indicative of the presence of uncoordinated triflate anions.[20–22] Further insight into the structure of [**1**](OTf) was obtained from its ESI-MS spectrum recorded in acetonitrile. Major ions were observed at m/z 295.99 and 740.94, corresponding to the dimeric cations $[Cu_2(L1)_2]^{2+}$ (calcd 296.03) and $[Cu_2(L1)_2(OTf)]^{+}$ (calcd 741.02), respectively. In addition, a signal observed at m/z 518.63 can be attributed to trinuclear copper species $[Cu_3(L1)_3(OTf)]^{2+}$ (calcd 518.53). The molar conductivity of 243 $cm^2\,mol^{-1}\,\Omega^{-1}$ for a 1 mM solution of [**1**](OTf) in acetonitrile lies in the reported range for 2:1 electrolytes.[23] In addition, a d–d transition was observed at 636 nm in the electronic spectrum of [**1**](OTf) in acetonitrile.

To obtain further insight into the structure of the 1:1 $Cu(OTf)_2$/L1 complex, EPR and magnetic properties were studied. The solid-state EPR spectrum showed broad, isotropic signals, which probably arise from exchange narrowing due to close proximity of Cu ions in the solid lattice. In solution, a complicated multispecies spectrum was obtained that included a signal derived from a dinuclear species. Variable-temperature magnetic susceptibility data were collected on a powdered sample. These data could not be fitted to a "simple" dinuclear species. Efforts to grow crystals of [**1**](OTf) suitable for X-ray crystallography have failed so far.

Although not conclusive, the above data suggest the presence of both dinuclear and higher nuclearity species. We therefore suggest the formation of a polynuclear structure through the initial formation of dimers followed by equilibrium polymerisation (Figure 2). Herein we will refer to the 1:1 complex of $Cu(OTf)_2$ and L1 as $[Cu(L1)]_n(OTf)_n$ or [**1**](OTf).

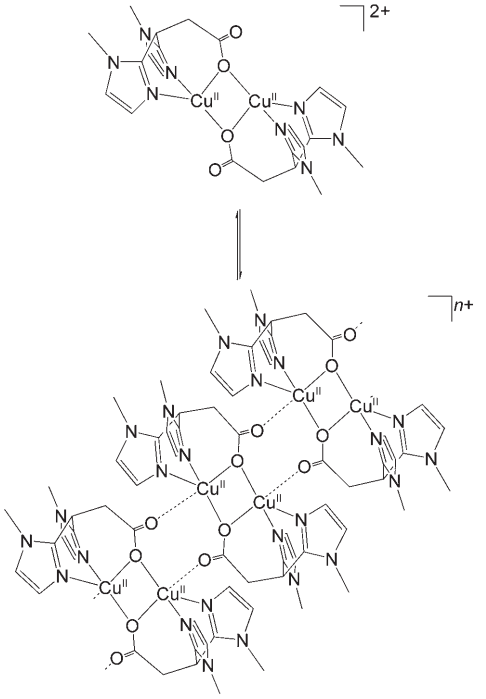

Figure 2. Proposed structure of the cationic part of [**1**](X) (X = OTf or PF_6): a polynuclear material formed from dinuclear units.

For solubility reasons, the triflate anion in [**1**](OTf) was exchanged for a PF_6^- anion by addition of an excess of potassium hexafluorophosphate to an aqueous solution of [**1**](OTf). The resulting light blue powder of $[Cu(L1)]_n(PF_6)_n$ ([**1**](PF_6)) has similar spectroscopic properties to [**1**](OTf), and hence, the same structural formulation is inferred. Unfortunately, numerous attempts to obtain single crystals of [**1**](PF_6) also failed.

Catecholase activity: The (partial) dinuclear character of [**1**](X) (X = OTf, PF_6) in solution prompted us to study the catecholase activity of these complexes in the oxidation of benchmark substrate 3,5-di-*tert*-butylcatechol (H_2dtbc) to 3,5-di-*tert*-butylbenzoquinone (dtbq) in acetonitrile. The product dtbq has a strong absorption band at about 395 nm, and therefore the reaction can be easily monitored by UV/Vis spectroscopy. Because [**1**](OTf) dissolves only very slowly in acetonitrile, the studies described below were performed with [**1**](PF_6). To estimate the catecholase-type activity of [**1**](PF_6), a solution of the catalyst in acetonitrile was treated with 25 equiv of H_2dtbc. Formation of dtbq was followed over time by UV/Vis spectroscopy (Figure 3).

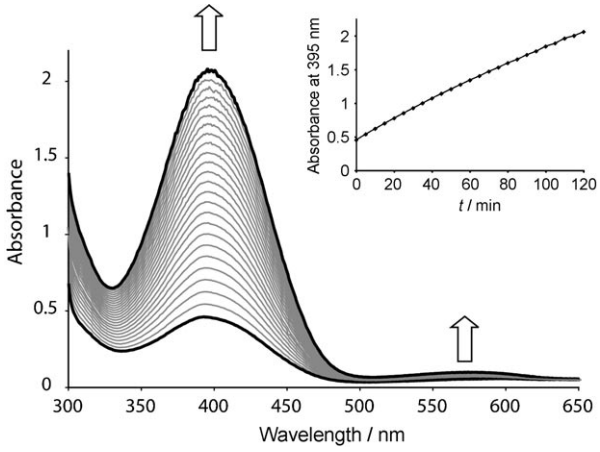

Figure 3. Oxidation of 3,5-di-*tert*-butylcatechol by [**1**](PF_6), monitored by UV/Vis spectroscopy. Spectra were recorded at regular time intervals (5 min) over a period of 120 min. The inset shows the increase in absorption at 395 nm with time.

The results show that [**1**](PF_6) does catalyse the oxidation of H_2dtbc, but only with a very modest activity (2.6 turnovers with respect to copper after 120 min). The activity was tested at different substrate concentrations. Michealis–Menten-type substrate saturation behaviour, which is commonly observed at higher substrate concentrations in related model studies,[2,3,24] was not observed and the reaction rate was found to be independent of substrate concentration over the range studied (5–50 equiv). This phenomenon has been observed before,[7,11,25] and particularly strong binding of the substrate to the catalyst was proposed as a possible explanation.[11]

Tetrachlorocatechol binding studies: The mode of binding of catechols to [**1**](PF_6) was studied by adding tetrachlorocatechol (H_2tcc) to a solution of [**1**](PF_6) in acetonitrile. Tetrachlorocatechol has a higher oxidation potential than H_2dtbc[26,27] due to its electron-withdrawing substituents and is commonly used as a pseudo-substrate resistant to oxidation. Upon titration of a solution of [**1**](PF_6) with H_2tcc, a new band appears at 430 nm and concomitantly the intensity of the d–d transition decreases (Figure 4).

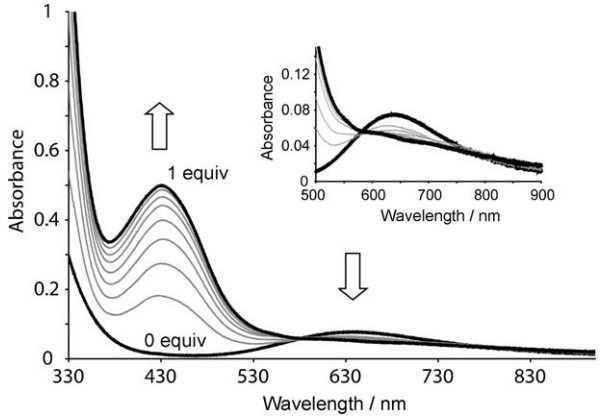

Figure 4. UV/Vis spectral changes upon addition of tetrachlorocatechol (0–1 equiv in 0.125 equiv increments) to a solution of [**1**](PF_6) in acetonitrile. Arrows indicate a decrease or increase in absorption upon addition. The inset shows the spectral changes in the d–d transition region.

The spectral changes correspond to the observed colour change of the solution from blue to yellow upon addition of H_2tcc. The two isosbestic points at 581 and 785 nm indicate the presence of only two absorbing species in solution. These marked changes are consistent with previously observed UV/Vis spectral changes upon titration of dinuclear copper(II) complexes with tetrachlorocatechol[2,28,29] and indicate binding of the catechol to the complex.

To obtain further insight into the binding mode of tetrachlorocatechol, we tried to obtain single crystals of the adduct. However, the crystallisation solutions gradually changed colour from yellow to brown to green over several weeks. A crystal structure determination on the green crystals that were obtained revealed that tetrachlorocatechol was no longer intact. Instead, a chloranilato (ca) moiety was found to bridge two copper(II) centres in $[Cu_2(ca)Cl_2(HL1)_2]$ (**2**; Figure 5).

Crystal structure of $[Cu^{II}_2(ca)Cl_2(HL1)_2]\cdot 8MeCN\cdot 2H_2O$: Green crystals of **2**·8MeCN·2H_2O suitable for X-ray diffraction were obtained from a solution of [**1**](PF_6) and one equivalent of tetrachlorocatechol (H_2tcc) in acetonitrile upon standing. The molecular structure of **2**·8MeCN·2H_2O is depicted in Figure 5, and selected bond lengths and angles are presented in Table 1. The crystal structure of **2**·8MeCN·2H_2O consists of discrete chloranilato bridged dimers in which the chloranilato dianion is located on an in-

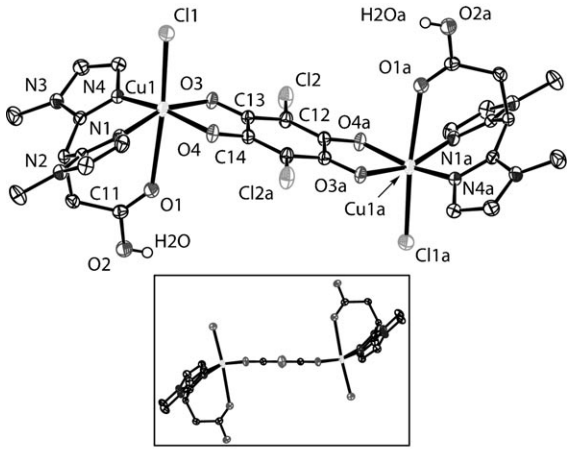

Figure 5. Molecular structure of $[Cu^{II}_2(ca)Cl_2(HL1)_2]\cdot 8MeCN\cdot 2H_2O$ in the crystal. All CH hydrogen atoms and co-crystallised acetonitrile and water solvent molecules have been omitted for clarity. Displacement ellipsoids are drawn at the 50% probability level. Symmetry operation a: $1-x, 1-y, 1-z$. The side view of the dimer in the inset shows the planarity of the bridging chloranilato dianion.

version centre and is bound as a bis-bidentate bridging ligand. Each copper(II) atom is facially capped by a protonated, neutral HL1 ligand. A chlorido anion completes the $N_2O_2O'Cl$ donor set to result in a severely distorted octahedral coordination geometry around each copper(II) centre. The basal plane is defined by the two nitrogen donor atoms and the chloranilato oxygen donor atoms. The copper atom lies 0.2713(2) Å above this plane towards the chlorido ligand. The complex is centrosymmetric with the crystallographic inversion centre coinciding with the centre of the chloranilato ring. The intramolecular Cu···Cu separation is 7.7628(5) Å. The chloranilato moiety is planar and its structural features are consistent with delocalisation of the negative charges to the lower and upper regions of the ring. This is reflected in the C12–C13 and C12a–C14 (1.393(2) and 1.398(2) Å) and the C13–O3 and C14–O4 bond lengths (1.2627(19) and 1.259(2) Å). The C13–C14 bond length of 1.530(2) Å is indicative of a single bond. All of these features result in essentially equal Cu–O distances and a symmetric binding mode of the dianion. Some end-capped dimeric $[Cu_2(ca)]$ structures have been reported before, and the observed bond lengths of the dicopper(II) chloranilato moiety in the structure of **2**·8MeCN·2H$_2$O compare well with the reported values.[30–34] These end-capped dinuclear complexes were all synthesised by self-assembly of their components, that is, they were obtained from mixtures of chloranilic acid, a copper(II) source, and a bi- or tridentate nitrogen donor ligand.

The neutral HL1 ligand is coordinated to copper through both 1-methylimidazole N donor atoms and the carbonyl O atom of the carboxyl group. This is supported by C–O bond lengths of 1.210(2) and 1.326(2) Å for C11–O1 and C11–O2, respectively, and involvement of O2 in a hydrogen-bonding interaction of the OH group of the acid with a co-crystallised water molecule (Figure 6). The $Cu-O_{carbonyl}$ distance in **2**·8MeCN·2H$_2$O (2.7911(12) Å) is much longer than the $Cu-O_{carboxylato}$ distance observed in the related complex $[Cu^{II}(L1)_2]\cdot 2H_2O$ (2.400 Å),[12] in which the monoanionic L1 ligand is coordinated through its carboxylato O anion. The two co-crystallised water molecules are involved in identical hydrogen-bonding patterns that connect the dimeric units into a one-dimensional ladder-like structure (Figure 6, Table 2).

The carboxylic acid proton H2O is involved in a hydrogen bond with oxygen atom O5 of a lattice water molecule. The water molecule is in turn involved in a hydrogen bond with a chlorido ligand of a second dinuclear unit. Finally, the water molecule forms an additional hydrogen bond with one of the co-crystallised acetonitrile molecules.

Chloranilic acid formation: The observed conversion of tetrachlorocatechol to chloranilic acid is very unusual. Because tetrachlorocatechol is stable in acetonitrile under ambient conditions, complex [**1**](PF$_6$) apparently mediates the stoichiometric oxidative dehalogenation of tetrachlorocatechol to chloranilic acid (Scheme 1). Both the protons and chloride anions that are released during the reaction can be found in the final product. The monoanionic ligands L1 are

Table 1. Selected bond lengths [Å] and angles [°] for **2**·8MeCN·2H$_2$O and **3**. Symmetry operation a: $1-x, 1-y, 1-z$.

2·8MeCN·2H$_2$O									
Cu1–Cl1	2.5171(5)	Cl1-Cu1-O1	174.62(3)	Cl1-Cu1-O3	96.99(4)	C11–O1	1.210(2)	C13–C12	1.393(2)
Cu1–N1	1.9607(14)	O3-Cu1-N1	161.09(6)	Cl1-Cu1-O4	95.53(4)	C11–O2	1.326(2)	C12–C14a	1.398(2)
Cu1–N4	1.9541(14)	O4-Cu1-N4	165.93(6)	Cl1-Cu1-N1	101.06(4)	C13–O3	1.2627(19)	C13–C14	1.530(2)
Cu1–O1	2.7911(12)	O1-Cu1-N1	77.88(5)	Cl1-Cu1-N4	97.59(4)	C14–O4	1.259(2)		
Cu1–O3	2.0234(12)	O1-Cu1-N4	77.19(5)	O4-Cu1-N1	91.85(5)				
Cu1–O4	2.0027(12)	O1-Cu1-O3	84.66(5)	N1-Cu1-N4	90.60(6)				
		O1-Cu1-O4	89.79(4)	N4-Cu1-O3	92.57(5)				
				O3-Cu1-O4	80.79(5)				
3									
Cu1–O1	2.302(2)	O1-Cu1-N11	91.35(9)	O22-Cu1-N11	166.99(9)	C12–O12	1.272(3)	C22–C32	1.390(4)
Cu1–N11	1.971(2)	O1-Cu1-N41	102.75(8)	O12-Cu1-N11	93.49(8)	C22–O22	1.267(3)	C32–C42	1.407(4)
Cu1–N41	1.950(2)	O1-Cu1-O22	101.11(8)	N11-Cu1-N41	90.85(9)	C52–O42	1.227(3)	C42–C52	1.550(4)
Cu1–O12	1.9485(19)	O1-Cu1-O12	88.56(8)	N41-Cu1-O22	90.03(8)	C42–O32	1.243(3)	C52–C62	1.418(4)
Cu1–O22	1.9700(19)	O12-Cu1-N41	167.80(9)	O22-Cu1-O12	83.21(8)	C12–C22	1.518(4)	C62–C12	1.375(4)

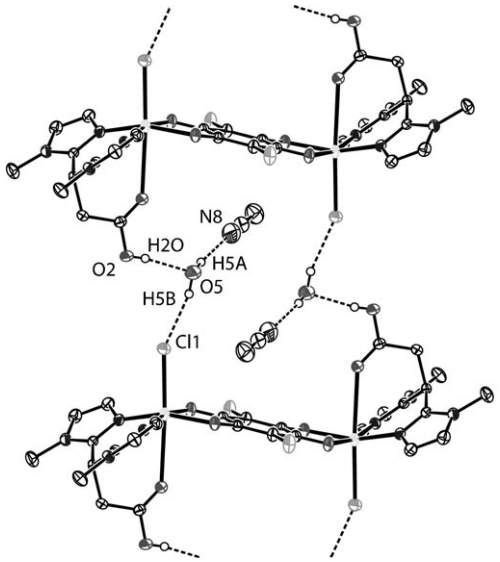

Figure 6. Hydrogen-bonding network of **2**·8 MeCN·2 H_2O resulting in a ladder-like structure. All CH hydrogen atoms and co-crystallised solvent molecules that do not participate in hydrogen bonding have been omitted for clarity.

Table 2. Selected hydrogen-bond lengths [Å] and angles [°] for **2**·8 MeCN·2 H_2O and **3**. Symmetry operations for **3**: i) $-x, -y, -z$; ii) $1-x, 1-y, 1-z$; iii) $1+x, 1+y, 1+z$.

Donor–H···Acceptor	D–H	H···A	D···A	D–H···A
	2·8 MeCN·2 H_2O			
O2–H2O···O5	0.73(3)	1.91(3)	2.627(2)	170(3)
O5–H5A···N8	0.93(3)	2.04(3)	2.932(3)	161(3)
O5–H5B···Cl1	0.87(3)	2.28(3)	3.1111(18)	159(3)
	3			
O1–H1O···O42^{i}	0.71(5)	2.05(5)	2.742(3)	166(5)
O1–H2O···O21^{ii}	0.85(5)	2.07(5)	2.919(3)	173(5)
O11–H11O ···O32^{iii}	0.96(5)	1.65(5)	2.594(3)	169(5)

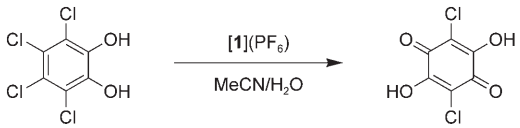

Scheme 1. Formation of chloranilic acid in the reaction of [**1**](PF_6) with tetrachlorocatechol.

coordinated as their conjugate acid HL1 and the chloride anions are each coordinated to one of the copper(II) ions of the dimer. The reaction can also be performed on a larger scale. Upon addition of tetrachlorocatechol to a blue solution of [**1**](PF_6) in acetonitrile/water (100/1 v/v), an immediate colour change to brown-yellow was observed and after stirring the reaction for a week under ambient conditions a green solution was obtained. The product was finally collected as a green crystalline solid in a yield of 41 %. It was analysed by elemental analysis and the spectroscopic data were compared with those of independently synthesised **2** (see below). No product is obtained when the reaction is performed under an argon atmosphere or under water-free conditions, that is, both water and dioxygen are required for formation of **2**.

Independent synthesis of [Cu^{II}_2(ca)Cl_2(HL1)$_2$] (2): Complex **2** can also be directly synthesised from its components. Addition of chloranilic acid to a solution containing equimolar amounts of $CuCl_2$·H_2O and [Bu_4N][L1] in methanol resulted in the precipitation and isolation of **2** as a dark green powder.

The IR spectrum of **2** is identical to that obtained for the product isolated from the reaction of [**1**](PF_6) and tetrachlorocatechol (see above). The carboxylato group of L1 is protonated upon formation of the complex, as indicated by the asymmetric stretching band at 1731 cm^{-1}. Bands at 1525 and 1383 cm^{-1} can be attributed to the chloranilato group and agree well with the approximate D_{2h} symmetry of this group.[30] The electronic absorption spectrum of a powder sample of **2**, which has a green colour, shows two absorptions at 403 and 629 nm, which can be attributed to a charge-transfer band and a d–d transition, respectively.[30]

The complex is insoluble in acetonitrile. Interestingly, dissolution of green complex **2** in methanol yielded a blue-purple solution, whereas in DMF a pinkish purple solution was obtained. Two bands are observed in the UV/Vis absorption spectrum of a solution of **2** in DMF: one at 518 nm ($\varepsilon = 725\ M^{-1}cm^{-1}$) and a less intense band at 679 nm ($\varepsilon = 150\ M^{-1}cm^{-1}$). The transition at 518 nm can be assigned to a chloranilato-to-copper charge-transfer transition of a chloranilato moiety with *ortho*-benzoquinone character.[30] Credence for this assignment and further insight into the structure of the pink-purple chromophore was obtained from an X-ray crystal structure determination on single crystals of [Cu(ca)(HL1)(H_2O)] (**3**), grown from a solution of **2** in acetonitrile/methanol (see below). Apparently, a new equilibrium of both mono- and dinuclear species is established upon dissolution of **2** that ultimately results in crystallisation of mononuclear complex **3**. Ions from both dinuclear and mononuclear species are observed in the ESI-MS spectrum of **2**. The higher extinction coefficient associated with the mononuclear pink-purple chromophore, however, causes the colouration of the solution.

Magnetic and EPR properties of 2: The EPR spectrum of a powder sample of independently synthesised **2** recorded at room temperature and at 77 K showed an anisotropic signal with $g_{\parallel} = 2.26$ and $g_{\perp} = 2.08$ (weighted average g value of 2.14). The spectrum does not show the hyperfine splitting normally observed for mononuclear copper(II), and no indications of triplet spectra, expected for isolated dinuclear copper(II), were seen. Apparently, relatively short intermolecular Cu···Cu distances are responsible for exchange narrowing, resulting in a pseudo-axial spectrum without hyperfine splitting.

To find out more about the presence and exchange coupling of this dinuclear species, variable-temperature magnetic susceptibility data were collected for a powdered sample

of **2** at 0.1 T in the temperature range of 2 to 300 K. The plot of $\chi_M T$ and χ_M versus temperature is shown in Figure 7.

The $\chi_M T$ product of **2** at 300 K is 0.76 $cm^3 K mol^{-1}$, which is within the range expected for the spin-only value for two

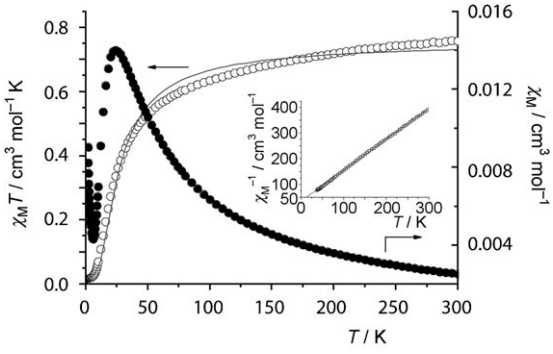

Figure 7. Plots of χ_M versus T (●) and $\chi_M T$ versus T (○) for **2** in the range of 2–300 K in 0.1 T field. The inset shows the plot of χ_M^{-1} versus T with the corresponding fitting.

non-interacting $S = {}^1/_2$ copper(II) centres with $g = 2$ (0.75 $cm^3 K mol^{-1}$). The value extrapolated to high T agrees with a g value of 2.14 (from EPR) and was used to fit the data for dinuclear copper(II). The $\chi_M T$ value decreases upon cooling, and the decrease is more pronounced from 65 K to 0.02 $cm^3 K mol^{-1}$ at 5 K; this behaviour is characteristic for antiferromagnetic coupling of the two copper(II) ions. The temperature dependence of the magnetic susceptibility of **2** was fitted to the Curie–Weiss expression with a C value of 0.83 $cm^3 K mol^{-1}$ and a θ value of -30 K. The negative θ value is again indicative of antiferromagnetic coupling between the metal centres.

The experimental $\chi_M T$ data were fitted to the equation for dinuclear copper compounds derived from the Hamiltonian $\mathscr{H} = J(\mathbf{S}_1 \cdot \mathbf{S}_2)$ [Eq. (1)]:[35]

$$\chi_i = \frac{\chi_i}{1-(2zJ'/Ng^2\beta^2)\chi_i}$$

in which χ_i is given by Equation (2):

$$\chi_i = (1-\rho)\frac{2N_A\beta^2 g^2}{k_B T}[3+\exp(-J/k_B T)]^{-1} + \rho\left(\frac{N_A g^2 \beta^2}{2k_B T}\right) + \mathrm{TIP}$$

in which zJ' covers the intermolecular interactions (between different dinuclear species), and χ_i is the magnetic susceptibility considering the paramagnetic impurities (ρ) and the temperature-independent paramagnetism (TIP) of the Cu^{II} ions. The fit shown in the graph was based on $g = 2.14$ (fixed from the EPR experimental data), $J = -35$ cm^{-1}, $zJ' = -0.1$ cm^{-1} and $\rho = 0.02$ (from a fit of the experimental data) with a reliability factor (R) of 4.6×10^{-4}. A TIP of 60×10^{-6} $cm^3 mol^{-1}$ (for each copper(II) ion) was taken into account. The negative J value arises from the antiferromagnetic interactions between the two metal centres and is typical for chloranilato-bridged dinuclear copper(II) complexes.[31,32,36]

Crystal structure of [Cu^{II}(ca)(HL1)(H_2O)] (3): Purple crystals of **3** suitable for X-ray diffraction were obtained from a blue-purple solution of **2** in acetonitrile/methanol upon standing. The molecular structure of **3** is depicted in Figure 8, and selected bond lengths and angles are presented in Table 1.

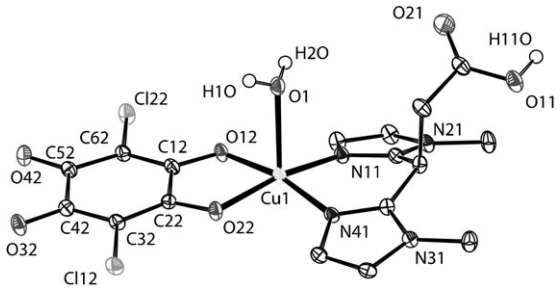

Figure 8. Molecular structure of [Cu^{II}(ca)(HL1)(H_2O)] (**3**) in the crystal. All CH hydrogen atoms have been omitted for clarity. Displacement ellipsoids are drawn at the 50% probability level.

The crystal structure consists of a mononuclear, five-coordinate copper(II) complex in which the dianionic chloranilato ligand acts as a bidentate terminal ligand. The protonated, neutral HL1 ligand is coordinated in an N,N-bidentate fashion to the copper centre through its 1-methylimidazole N donor atoms. The acid group is pointing away from the metal centre, that is, it is uncoordinated, and is involved in hydrogen-bonding interactions (see below). Completion of the coordination sphere around the copper ion by a water molecule results in an N_2O_2O' donor set. The coordination geometry around the metal centre is slightly distorted square-pyramidal with a τ value[37] of 0.01. The basal plane is made up of the two chloranilato oxygen atoms and the two nitrogen donor atoms of the HL1 ligand. The water molecule occupies the apical position. The copper atom is displaced 0.2024(3) Å from the best least-squares plane through the equatorial atoms towards the water molecule. The slight distortion from ideal symmetry is illustrated by the increased O1-Cu1-N41 and O1-Cu1-O22 angles (102.75(8) and 101.11(8)°, respectively). This is the result of the involvement of the water molecule in two hydrogen-bonding interactions, which move the oxygen atom slightly from the centre of the pyramid. The structural features of **3** compare well to those reported for [Cu^{II}(ox)(Hbip)(H_2O)],[38] which features the related 3,3-bis(imidazol-2-yl)-propionate (Hbip) ligand and has an oxalato (ox) group as the other bidentate, dianionic ligand. Similar Cu–N and Cu–OH_2 distances are found in both complexes.

As a result of the different binding modes of the chloranilato anion, that is, terminal bidentate in **3** versus bis-bidentate in **2**, the observed sequences of C–C and C–O bond lengths are different. The C–O bond lengths in **3** are

1.272(3) (C12–O12) and 1.267(3) Å (C22–O22) for the coordinated (anionic) oxygen atoms and 1.227(3) (C52–O42) and 1.243(3) Å (C42–O32) for the uncoordinated (carbonyl) oxygen atoms. The C–C single-bond lengths observed for C12–C22 and C42–C52 together with the intermediate C–C distances for the other C–C bond lengths in the chloranilato ring indicate charge delocalisation over the lower and upper regions of the ring. These structural features are similar to those observed in the few other reported copper complexes with a terminal bidentate chloranilato ligand.[30,33,39–41]

Three different hydrogen-bonding interactions are observed in the crystal structure of **3** (Table 2, Figure 9). The carboxyl oxygen atom of HL1 acts as a hydrogen-bond donor to uncoordinated chloranilato oxygen atom O32 of a second monomeric unit, and in this way an infinite, ladder-like linear chain is formed along the [1,1,1] body diagonal. The infinite linear chain is connected by two hydrogen bonds to a second infinite chain. The water molecule acts as a donor for two single hydrogen bonds to both the carbonyl oxygen atom O21 of the acid group and the other uncoordinated chloranilato oxygen atom O42. The two linear chains run antiparallel to each other, and the strand is further held together by a π–π stacking interaction between the chloranilato rings with an interplanar distance of 3.49 Å.

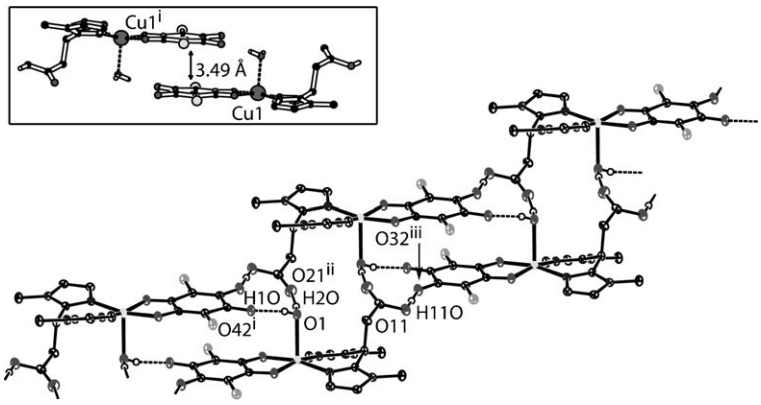

Figure 9. Hydrogen-bonding network of **3** resulting in infinite strands; all CH hydrogen atoms have been omitted for clarity. Inset: π–π stacking in the crystal structure of **3**. Symmetry operations: i) $-x$, $-y$, $-z$; ii) $1-x$, $1-y$, $1-z$; iii) $1+x$, $1+y$, $1+z$.

Discussion

The copper(II) coordination chemistry of ligand L1 and the reactivity with tetrachlorocatechol is summarised in Scheme 3.

Isolation of a chloranilato-bridged dinuclear copper(II) complex from a reaction mixture containing [**1**](PF_6) and tetrachlorocatechol was unexpected and is very unusual. In fact, the observed oxidative dehalogenation is, to the best of our knowledge, the first report of this type of chemical degradation of tetrachlorocatechol. Dehalogenation has been reported in reactions of Cu^I complexes with tetrachlorobenzoquinone. Chlorido-bridged dinuclear Cu^{II} complexes were found as one of the products in these reactions.[42,43] These conversions are the consequence of the well-established instability of tetrachlorobenzoquinone with respect to both reduction and dehalogenation.[17,44,45] The principal products of this conversion are tetrachlorocatechol and chloranilic acid. In contrast to tetrachlorobenzoquinone, tetrachlorocatechol is commonly used as a chemically inert catechol derivative because of its stability with respect to oxidation. Indeed, the formation of stable complexes with this electronically deactivated (pseudo)-substrate has been used to advantage in modelling studies.[11,42,46] The downside of this chemical stability is limited biodegradation of tetrachlorocatechol.

A plausible mechanism for the transformation of tetrachlorocatechol to chloranilic acid involves its initial oxidation to tetrachlorobenzoquinone by [**1**](PF_6) (Scheme 2). Subsequently, two consecutive nucleophilic attacks of water result in dehalogenation and formation of chloranilic acid with release of two equivalents of HCl. In the presence of dioxygen the Cu^I ions formed in the first step are reoxidised to Cu^{II}, and dimeric complex **2** can be assembled. Importantly, the chloranilic acid product has low acute toxicity and is unlikely to pose a major environmental threat.[17] Further development of the stoichiometric reaction reported herein might provide a new method for the chemical oxidation and dechlorination of halogenated aromatic compounds in waste-treatment and remediation processes.[47–49]

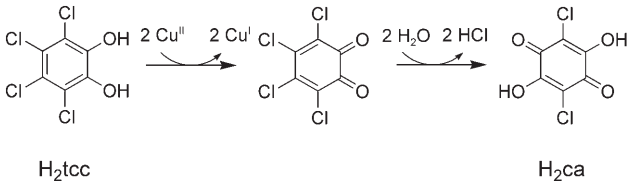

Scheme 2. Proposed mechanism for the degradation of tetrachlorocatechol (H_2tcc) to chloranilic acid (H_2ca).

Interestingly, a biological precedent is known for the observed formation of chloranilic acid from tetrachlorocatechol. The lignin-degrading white-rot fungus *Coriolus versicolour* converts tetrachloroguaiacol to tetrachlorocatechol and finally degrades the latter to, amongst other products, chloranilic acid.[16] The enzyme that is thought to be involved in this transformation is laccase. Laccase has a so-called type-4 copper active site,[2] which comprises a trinuclear copper cluster that is composed of a type-2 mononu-

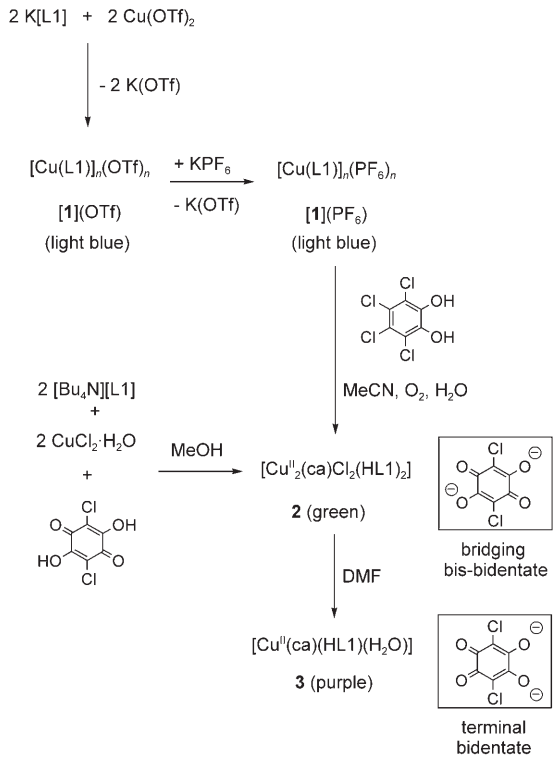

Scheme 3. Synthesis and reactivity of copper complexes **1**–**3**.

clear and type-3 dinuclear copper site. In this light, the reactivity of [**1**](PF$_6$) towards tetrachlorocatechol can be regarded as a functional model of the laccase involved in the dechlorination of tetrachlorocatechol.

Conclusion

The partial dinuclear character in solution of [**1**](X) (X= OTf, PF$_6$), which was obtained from the reaction of stoichiometric amounts of K[L1] and Cu(OTf)$_2$ followed by anion exchange for the PF$_6$ salt, prompted us to study its catecholase activity. Although the catecholase activity is modest, a different and surprising conversion of tetrachlorocatechol to chloranilic acid was discovered. Structure determination on single crystals obtained from a solution containing tetrachlorocatechol and dinuclear [**1**](PF$_6$) revealed formation of a dinuclear copper compound containing a bridging bis-bidentate chloranilato ligand. This ligand results from stoichiometric oxidative double dehalogenation of tetrachlorocatechol by a homogeneous copper complex to yield chloranilic acid. This conversion is unprecedented and provides an interesting new opportunity for the degradation of persistent organic pollutants, such as polychlorinated aromatic hydrocarbons. Furthermore, the supporting ligand HL1 shows flexible coordination chemistry, which ranges from N$_2$O binding as a monoanionic ligand in [**1**](PF$_6$), through N$_2$O(H) binding as a neutral ligand in [Cu$_2$(ca)Cl$_2$(HL1)$_2$] (**2**), to bidentate N$_2$ binding in [Cu(ca)(HL1)(H$_2$O)] (**3**).

Experimental Section

Infrared spectra were recorded with a Perkin–Elmer Spectrum One FTIR instrument. Elemental microanalyses were carried out by the Microanalytisches Laboratorium Dornis & Kolbe, Mulheim a.d. Ruhr (Germany). ESI-MS spectra were recorded on a Micromass LC-TOF mass spectrometer at the Biomolecular Mass Spectrometry group, Utrecht University. Solution UV/Vis spectra were recorded on a Varian Cary 50, and diffuse reflectance UV/Vis spectra on a Perkin–Elmer Lambda 900. Magnetic susceptibility measurements (2–300 K) were carried out with a Quantum Design MPMS-5 5T SQUID magnetometer at 0.1 T. Data were corrected for the magnetisation of the sample holder and for diamagnetic contributions, which were estimated from Pascal constants. X-band powder EPR spectra were obtained on polycrystalline samples with a JEOL RE2X EPR spectrophotometer with 2,2-diphenyl-1-picrylhydrazyl (DPPH, g=2.0036) as reference. The potassium and tetrabutylammonium salts of 3,3-bis(1-methylimidazol-2-yl)propionate (L1) were prepared according to a published procedure.[12] Tetrachlorocatechol was recrystallised from toluene before use. All other chemicals were obtained commercially and used as received. All concentrations of the solutions and the equivalents added in the reactivity and binding studies were calculated and are expressed with respect to the quantity of copper ions in solution.

[Cu(L1)]$_n$(OTf)$_n$ ([1](OTf)): A solution of Cu(OTf)$_2$ (384 mg, 1.06 mmol) in dry methanol (5 mL) was added to a solution of K[L1] (289 mg, 1.06 mmol) in warm, dry methanol (10 mL), and the resulting deep blue solution was stirred at 50 °C for 30 min, during which a light blue precipitate formed. The suspension was allowed to cool to room temperature and was stirred overnight, after which the blue precipitate was separated by centrifugation. The precipitate was washed with dry methanol (2× 20 mL) and the product was obtained as a blue powder (391 mg, 82 %). IR (solid): $\tilde{\nu}$=3139.2, 2963.8, 1555.5, 1516.2, 1433.6, 1412.4, 1320.0, 1258.4, 1223.8, 1148.0, 1028.3, 958.9, 768.9, 752.9 cm^{-1}; UV/Vis (acetonitrile): λ_{max} (ε)=636 nm (100 M^{-1}cm^{-1}); Conductivity (1 mM in acetonitrile): λ_M=243 cm^{2}mol$^{-1}\Omega^{-1}$; ESI-MS: m/z: 295.99 {[Cu$_2$(L1)$_2$]$^{2+}$, calcd 296.03}, 445.98 {[Cu(L1)(OTf)+H]$^+$, calcd 445.99}, 518.63 {[Cu$_3$(L1)$_3$-(OTf)]$^{2+}$, calcd 518.53}, 740.94 {[Cu$_2$(L1)$_2$(OTf)]$^+$, calcd 741.02}, 1186.30 {[Cu$_3$(L1)$_3$(OTf)$_2$]$^+$, calcd 1186.00}; elemental analysis calcd (%) for C$_{12}$H$_{13}$CuF$_3$N$_4$O$_5$S (445.86): C 32.33, H 2.94, N 12.57; found: C 32.46, H 3.10, N 12.38.

[Cu(L1)]$_n$(PF$_6$)$_n$ ([1](PF$_6$)): A solution of KPF$_6$ (840 mg, 5 equiv) in water (10 mL) was added to a blue solution of [**1**](OTf) (408 mg, 0.92 mmol) in water (35 mL), and immediately a light blue precipitate formed. The suspension was stirred for 10 min and the light blue precipitate was separated by centrifugation. The precipitate was washed with water (3×20 mL) and the product was obtained as a light blue powder (365 mg, 90 %). IR (solid): $\tilde{\nu}$=3157.1, 2962.0, 1555.1, 1527.2, 1515.8, 1433.1, 1411.0, 1320.2, 1289.1, 1213.8, 1171.4, 1148.9, 1092.4, 976.1, 958.4, 837.1, 818.7, 767.6, 742.8 cm^{-1}; UV/Vis (acetonitrile): λ_{max} (ε)=639 nm (100 M^{-1}cm^{-1}); conductivity (1 mM in acetonitrile): λ_M= 231 cm^{2}mol$^{-1}\Omega^{-1}$; ESI-MS: m/z: 296.00 {[Cu$_2$(L1)$_2$]$^{2+}$, calcd 296.03}, 737.03 {[Cu$_2$(L1)$_2$(PF$_6$)]$^+$, calcd 737.03}, 1052.06 {[Cu$_3$(L1)$_3$(PF$_6$)+F]$^+$, calcd 1052.06}; elemental analysis calcd (%) for C$_{11}$H$_{13}$CuF$_6$N$_4$O$_2$P (441.76): C 29.91, H 2.97, N 12.68; found: C 29.82, H 3.10, N 12.54.

[Cu$_2$(ca)Cl$_2$(HL1)$_2$] (2): A solution of tetrachlorocatechol (H$_2$tcc) (22 mg, 0.09 mmol) in acetonitrile/water (5 mL, 100:1 v/v) was added to a blue solution of [**1**](PF$_6$) (77 mg, 0.17 mmol) in acetonitrile (6 mL), and an immediate colour change to yellow-brown was observed. The solution was stirred for 8 d at room temperature, during which time the colour gradually changed from yellow-brown to green. The solution was filtered and concentrated to 3 mL. Green crystals of composition [Cu$_2$(ca)Cl$_2$-(HL1)$_2$]·6H$_2$O grew upon standing for several weeks (35 mg, 41 %). IR (solid): $\tilde{\nu}$=3419.7, 3135.3, 1732.0, 1522.2, 1504.6, 1383.4, 1286.0, 1148.3, 756.2 cm^{-1}; elemental analysis calcd (%) for C$_{28}$H$_{28}$Cu$_2$Cl$_4$N$_8$O$_8$·6H$_2$O (981.57): C 34.26, H 4.11, N 11.42; found: C 34.65, H 4.26, N 11.65.

Direct synthesis of [Cu$_2$(ca)Cl$_2$(HL1)$_2$] (2): CuCl$_2$·H$_2$O (157 mg, 0.92 mmol) was added to a colourless solution of [Bu$_4$N][L1] (438 mg, 0.92 mmol) in methanol (15 mL), and the blue solution was stirred for

5 min. A red solution of chloranilic acid (98 mg, 0.46 mmol) in methanol (5 mL) was added to this solution, and an immediate colour change to dark blue-green was observed. The solution was stirred overnight at room temperature, during which time a green precipitate gradually formed. The crude product was separated by centrifugation and washed with methanol (3×5 mL) and diethyl ether (3×20 mL). The product was obtained as a dark green powder (354 mg, 88%). IR (solid): $\tilde{\nu}$=3144.3, 3102.4, 2961.3, 1730.7, 1525.9, 1505.3, 1383.8, 1290.5, 1178.1, 1151.2, 1136.1, 861.3, 784.4 cm^{-1}; UV/Vis (DMF): λ_{max} (ε)=518 (725), 679 nm (150 $M^{-1}cm^{-1}$). UV/Vis (diffuse reflectance): λ_{max}=403, 629 nm; ESI-MS: *m/z*: 400.03 {$[Cu_2(ca)(HL1)_2]^{2+}$, calcd 400.00}, 504.00 {$[Cu(ca)(HL1)+H]^+$, calcd 503.97}, 799.13 {$[Cu_2(ca)(L1)_2+H]^+$, calcd 798.99}; elemental analysis calcd (%) for $C_{28}H_{28}Cu_2Cl_4N_8O_8$ (873.47): C 38.50, H 3.23, N 12.83; found: C 38.64, H 3.28, N 12.72.

Catecholase activity and tetrachlorocatechol titrations: A solution containing 5, 10, 25 or 50 equiv of 3,5-di-*tert*-butylcatechol in acetonitrile (0.1 mL) was added to a solution of [**1**](OTf) or [**1**](PF_6) in acetonitrile (2 mL, 0.75 mM) in a quartz cuvette. Upon addition of the substrate the blue solution immediately turned yellow. Quinone formation was monitored by recording the characteristic absorption at 395 nm. The reactions were performed under ambient conditions.

The titrations of [**1**](OTf) and [**1**](PF_6) with tetrachlorocatechol were performed by incremental additions of 10 μL aliquots of a 37.5 mM solution of tetrachlorocatechol in acetonitrile (0.125 equiv) to a solution of the copper(II) complex in acetonitrile (1.5 mM, 2 mL). UV/Vis spectra were recorded after each addition.

X-ray crystal structure determination of 2·8MeCN·2H$_2$O and 3: Reflections were measured on a Nonius Kappa CCD diffractometer with rotating anode (graphite monochromator, λ=0.71073 Å) up to a resolution of $\sin(\theta/\lambda)_{max}$=0.65 $Å^{-1}$. Intensities were integrated with EvalCCD[50] using an accurate description of the experimental setup for the prediction of the reflection contours. The structures were refined with SHELXL-97[51] against F^2 of all reflections. Non-hydrogen atoms were refined with anisotropic displacement parameters. All hydrogen atoms were located in the difference Fourier map. The OH hydrogen atoms were refined freely with isotropic displacement parameters; all other hydrogen atoms were refined with a riding model. Geometry calculations and checking for higher symmetry were performed with the PLATON program.[52]

X-ray crystal structure determination of 2·8MeCN·2H$_2$O: $C_{28}H_{28}Cl_4Cu_2N_8O_8$·8MeCN·2$H_2O$; M_W=1237.93; green block; 0.24×0.21×0.18 mm; monoclinic; $P2_1/c$ (no. 14); *a*=10.1857(4), *b*=11.0587(3), *c*=27.1239(14) Å; β=109.560(2)°; *V*=2878.9(2) $Å^3$; *Z*=2; ρ_{calcd}=1.428 $g\,cm^{-3}$; μ=0.99 mm^{-1}. 55363 reflections were measured at 150 K, corrected for absorption, and scaled on the basis of multiple measured reflections with the program SADABS[53] (correction range 0.79–0.84). 6601 reflections were unique (R_{int}=0.0418). The structure was solved with the program DIRDIF-99[54] by using automated Patterson methods. 361 parameters were refined with no restraints. *R*1/*wR*2 [$I>2\sigma(I)$]: 0.0299/0.0745. *R*1/*wR*2 (all reflections): 0.0398/0.0789. *S*=1.040. Residual electron density −0.33/0.51 e $Å^{-3}$.

X-ray crystal structure determination of 3: $C_{17}H_{16}Cl_2CuN_4O_7$; M_W=522.78; dark purple block; 0.30×0.30×0.15 mm; triclinic; $P\bar{1}$ (no. 2); *a*=7.6753(3), *b*=11.5330(4), *c*=12.0878(4) Å; α=111.707(2), β=101.398(2), γ=90.896(1)°; *V*=969.88(6) $Å^3$; *Z*=2; ρ_{calcd}=1.790 $g\,cm^{-3}$; μ=1.45 mm^{-1}. 13998 reflections were measured at 110 K. The crystal appeared to be non-merohedrally twinned with a twofold rotation about the crystallographic *b* axis as twin operation. This twin operation was taken into account during integration of the intensities and HKLF5 refinement.[55] An absorption correction was not applied due to the twinning. 4424 reflections were unique (R_{int}=0.0676). The structure was solved for non-overlapping reflections with the program DIRDIF-99[54] by using automated Patterson methods. 295 parameters were refined with no restraints. *R*1/*wR*2 [$I>2\sigma(I)$]: 0.0390/0.0975. *R*1/*wR*2 (all reflections): 0.0434/0.1002. *S*=1.177. The twin fraction refined to 0.371(3). Residual electron density −0.72/0.62 e $Å^{-3}$.

CCDC-634539 (**2**·8MeCN·2H_2O) and 634540 (**3**) contain the supplementary crystallographic data for this paper. These data can be obtained free of charge from The Cambridge Crystallographic Data Centre via www.ccdc.cam.ac.uk/data_request/cif.

Acknowledgements

The work described here was financially supported by the National Research School Combination-Catalysis (P.C.A.B.) and the Council for Chemical Sciences of the Netherlands Organization for Scientific Research (CW-NWO) (M.L., A.L.S.). Dr. Stefania Tanase-Grecea is kindly acknowledged for her help with the magnetic measurements. Support from the FP6 Network of Excellence "Magmanet" (contract number 515767) to J.R. is also kindly acknowledged.

[1] E. I. Solomon, P. Chen, M. Metz, S.-K. Lee, A. E. Palmer, *Angew. Chem.* **2001**, *113*, 4702–4724; *Angew. Chem. Int. Ed.* **2001**, *40*, 4570–4590.
[2] I. A. Koval, P. Gamez, C. Belle, K. Selmeczi, J. Reedijk, *Chem. Soc. Rev.* **2006**, *35*, 814–840.
[3] T. Klabunde, C. Eicken, J. C. Sacchettini, B. Krebs, *Nat. Struct. Biol.* **1998**, *5*, 1084–1090.
[4] Y. Matoba, T. Kumagai, A. Yamamoto, H. Yoshitsu, M. Sugiyama, *J. Biol. Chem.* **2006**, *281*, 8981–8990.
[5] A. Volbeda, W. G. Hol, *J. Mol. Biol.* **1989**, *209*, 249–279.
[6] C.-T. Yang, M. Vetricheivan, X. Yang, B. Moubaraki, K. S. Murray, J. J. Vittal, *Dalton Trans.* **2004**, 113–121.
[7] K. Selmeczi, M. Réglier, M. Giorgi, G. Speier, *Coord. Chem. Rev.* **2003**, *245*, 191–201.
[8] M. Merkel, N. Möller, M. Piacenza, S. Grimme, A. Rompel, B. Krebs, *Chem. Eur. J.* **2005**, *11*, 1201–1209.
[9] I. A. Koval, K. Selmeczi, C. Belle, C. Philouze, E. Saint-Aman, I. Gautier-Luneau, A. M. Schuitema, M. van Vliet, P. Gamez, O. Roubeau, M. Lüken, B. Krebs, M. Lutz, A. L. Spek, J.-L. Pierre, J. Reedijk, *Chem. Eur. J.* **2006**, *12*, 6138–6150.
[10] A. Granata, E. Monzani, L. Casella, *J. Biol. Inorg. Chem.* **2004**, *9*, 903–913.
[11] J. Ackermann, F. Meyer, E. Kaifer, H. Pritzkow, *Chem. Eur. J.* **2002**, *8*, 247–258.
[12] P. C. A. Bruijnincx, M. Lutz, A. L. Spek, E. L. van Faassen, B. M. Weckhuysen, G. van Koten, R. J. M. Klein Gebbink, *Eur. J. Inorg. Chem.* **2005**, 779–787.
[13] K. Kervinen, P. C. A. Bruijnincx, A. M. Beale, J. G. Mesu, G. van Koten, R. J. M. Klein Gebbink, B. M. Weckhuysen, *J. Am. Chem. Soc.* **2006**, *128*, 3208–3217.
[14] P. C. A. Bruijnincx, I. L. C. Buurmans, S. Gosiewska, M. Lutz, A. L. Spek, G. van Koten, R. J. M. Klein Gebbink, *Chem. Eur. J.* **2008**, *14*, 1228–1237.
[15] P. C. A. Bruijnincx, M. Lutz, A. L. Spek, W. R. Hagen, B. M. Weckhuysen, G. van Koten, R. J. M. Klein Gebbink, *J. Am. Chem. Soc.* **2007**, *129*, 2275–2286.
[16] Y. Iimura, P. Hartikainen, K. Tatsumi, *Appl. Microbiol. Biotechnol.* **1996**, *45*, 434–439.
[17] M. Remberger, P.-Å. Hynning, A. H. Neilson, *Environ. Sci. Technol.* **1991**, *25*, 1903–1907.
[18] P. C. A. Bruijnincx, M. Lutz, J. P. den Breejen, A. L. Spek, G. van Koten, R. J. M. Klein Gebbink, *J. Biol. Inorg. Chem.* **2007**, *12*, 1181–1196.
[19] G. B. Deacon, R. J. Phillips, *Coord. Chem. Rev.* **1980**, *33*, 227–250.
[20] S. P. Gejji, K. Hermansson, J. Lindgren, *J. Phys. Chem.* **1993**, *97*, 3712–3715.
[21] S. Gosiewska, J. L. M. Cornelissen, M. Lutz, A. L. Spek, G. van Koten, R. J. M. Klein Gebbink, *Inorg. Chem.* **2006**, *45*, 4214–4227.
[22] D. H. Johnston, D. F. Shriver, *Inorg. Chem.* **1993**, *32*, 1045–1047.
[23] W. J. Geary, *Coord. Chem. Rev.* **1971**, *7*, 81–122.
[24] A. Rompel, H. Fischer, D. Meiwes, K. Büldt-Karentzopoulos, R. Dillinger, F. Tuczek, H. Witzel, B. Krebs, *J. Biol. Inorg. Chem.* **1999**, *4*, 56–63.

[25] E. Monzani, L. Quinti, A. Perotti, L. Casella, M. Gullotti, L. Randaccio, S. Geremia, G. Nardin, P. Faleschini, G. Tabbì, *Inorg. Chem.* **1998**, *37*, 553–562.
[26] M. D. Stallings, M. M. Morrison, D. T. Sawyer, *Inorg. Chem.* **1981**, *20*, 2655–2660.
[27] S. Harmalker, S. E. Jones, D. T. Sawyer, *Inorg. Chem.* **1983**, *22*, 2790–2794.
[28] J. Reim, B. Krebs, *J. Chem. Soc. Dalton Trans.* **1997**, 3793–3804.
[29] S. Torelli, C. Belle, S. Hamman, J.-L. Pierre, E. Saint-Aman, *Inorg. Chem.* **2002**, *41*, 3983–3989.
[30] J. V. Folgado, R. Ibáñez, E. Coronado, D. Beltrán, J.-M. Savariault, J. Galy, *Inorg. Chem.* **1988**, *27*, 19–26.
[31] C. Fujii, M. Mitsumi, M. Kodera, K.-I. Motoda, M. Ohba, N. Matsumoto, H. Okawa, *Polyhedron* **1994**, *13*, 933–938.
[32] S. Gallert, T. Weyhermüller, K. Wieghardt, P. Chaudhuri, *Inorg. Chim. Acta* **1998**, *274*, 111–114.
[33] M. Kawahara, M. K. Kabir, K. Yamada, K. Adachi, H. Kumagai, Y. Narumi, K. Kindo, S. Kitagawa, S. Kawata, *Inorg. Chem.* **2004**, *43*, 92–100.
[34] C. G. Pierpont, L. C. Francesconi, D. N. Hendrickson, *Inorg. Chem.* **1977**, *16*, 2367–2376.
[35] O. Kahn, *Molecular Magnetism*, Wiley-VCH, New York, **1993**.
[36] P. Chaudhuri, K. Oder, *J. Chem. Soc. Dalton Trans.* **1990**, 1597–1605.
[37] A. W. Addison, T. N. Rao, J. Reedijk, J. van Rijn, G. C. Verschoor, *J. Chem. Soc. Dalton Trans.* **1984**, 1349–1356.
[38] Y. Akhriff, J. Server-Carrió, A. Sancho, J. García-Lozano, E. Escrivá, J. V. Folgado, L. Soto, *Inorg. Chem.* **1999**, *38*, 1174–1185.
[39] L.-M. Zheng, H. W. Schmalle, S. Ferlay, S. Decurtins, *Acta Cryst. Sect. C* **1998**, *54*, 1578–1580.
[40] S. Reinoso, P. Vitoria, L. San Felices, L. Lezama, J. Gutiérrez-Zorilla, *Acta Cryst. Sect. E* **2005**, *61*, m1925 m1927.
[41] S. Kawata, H. Kumagai, K. Adachi, S. Kitagawa, *J. Chem. Soc. Dalton Trans.* **2000**, 2409–2417.
[42] H. Börzel, P. Comba, H. Pritzkow, *Chem. Commun.* **2001**, 97–98.
[43] E. H. Alilou, M. Giorgi, M. Pierrot, M. Reglier, *Acta Cryst. Sect. C* **1992**, *48*, 1612–1614.
[44] M. Remberger, P.-Å. Hynning, A. H. Neilson, *Ecotoxicol. Environ. Saf.* **1991**, *22*, 320–336.
[45] X. Fang, H.-P. Schuchmann, C. von Sonntag, *J. Chem. Soc. Perkin Trans. 2* **2000**, 1391–1398.
[46] K. D. Karlin, Y. Gultneh, T. Nicholson, J. Zubieta, *Inorg. Chem.* **1985**, *24*, 3727–3729.
[47] A. Sorokin, J.-L. Séris, B. Meunier, *Science* **1995**, *268*, 1161–1166.
[48] S. Sen Gupta, M. Stadler, C. A. Noser, A. Ghosh, B. Steinhoff, D. Lenoir, C. P. Horwitz, K.-W. Schramm, T. J. Collins, *Science* **2002**, *296*, 326–328.
[49] G. Lente, J. H. Espenson, *Green Chem.* **2005**, *7*, 28–34.
[50] A. J. M. Duisenberg, L. M. J. Kroon-Batenburg, A. M. M. Schreurs, *J. Appl. Crystallogr.* **2003**, *36*, 220–229.
[51] G. M. Sheldrick, SHELXL-97, Program for crystal structure refinement, University of Göttingen, Göttingen (Germany), **1997**.
[52] A. L. Spek, *J. Appl. Crystallogr.* **2003**, *36*, 7–13.
[53] G. M. Sheldrick, SADABS: Area-Detector Absorption Correction, V2.10, University of Göttingen, Göttingen (Germany), **1999**.
[54] P. T. Beurskens, G. Admiraal, G. Beurskens, W. P. Bosman, S. Garcia-Granda, R. O. Gould, J. M. M. Smits, C. Smykalla, The DIRDIF99 program system, Technical Report of the Crystallography Laboratory, University of Nijmegen, The Netherlands, **1999**.
[55] R. Herbst-Irmer, G. M. Sheldrick, *Acta Cryst. Sect. B* **1998**, *54*, 443–449.

Received: November 28, 2007
Published online: April 30, 2008

